Applied Energy 280 (2020) 115973

Contents lists available at ScienceDirect

Applied Energy

journal homepage: www.elsevier.com/locate/apenergy

An advanced day-ahead bidding strategy for wind power producers considering confidence level on the real-time reserve provision

Seyyed Ahmad Hosseini *, Jean-François Toubeau, Zacharie De Grève, François Vallée

Electrical Power Engineering Unit (EPEU), Power Systems & Market Research Group, University of Mons, 7000 Mons, Belgium

HIGHLIGHTS

- Wind power bidding in energy and reserve market respecting reliability of reserve bid.
- The proposed model is recast in a tractable mixed-integer linear programming approach.
- Impact of wind fluctuations on portfolio's profit and reserve confidence are evaluated ex-post.

ARTICLE INFO

Keywords:
Bidding strategy
Energy and reserve market
Chance-constrained programming
Stochastic optimization
Wind turbulence intensity

ABSTRACT

The current evolutions in electricity market policies combined with the technical progress in wind farm control encourage Wind Power Producers (WPPs) to participate in the joint day-ahead energy and reserve market (JERM). In this paper, an advanced bidding strategy dedicated to optimal dispatch of the WPP in the JERM is proposed. The suggested strategy exploits a novel bi-objective two-stage chance-constrained stochastic model in which various revenue streams, stemming from both day-ahead and real-time stages, are fully accounted for. The first objective of the presented model is to allocate the optimal share of the power assigned to each market floor in the day-ahead stage so as to maximize the WPP's profit. Then, the formulation considers the confidence level of delivering the contracted reserve power in real-time through an additional competing objective. Meanwhile, the presented method allows us to also illustrate the effect of reserve availability as a probabilistic measure on WPP's profit. In this regard, the wind speed and system frequency uncertainties are introduced as stochastic inputs in the proposed framework. The obtained revenue streams regarding each market floor as well as the total revenue of the WPP are then evaluated in a Monte Carlo out-of-sample analysis. The ex-post samples contain system frequency data from the Belgian market along with wind speed data representing the wind turbulence intensity level. Outcomes reveal not only the effectiveness and flexibility of the proposed model for enhancing WPPs' revenues, but also the importance of properly considering the uncertain real-time delivery of the contracted reserve power.

1. Introduction

Liberalization of the electricity market exposed new challenges for secure and reliable operation of the power systems compared to the former vertically integrated structure Therefore, other market floors such as the day-ahead reserve market are complementing the day-ahead energy market so as to help compensating for the real-time mismatch between generation and demand, thereby improving the dynamic aspects of the power systems [1]. These market floors are accompanied by a real-time balancing stage in which the imbalances from the scheduled bids are financially settled [2].

Meanwhile, the recent worldwide rising investment in renewable energy projects such as large wind power plants indicates a broad expansion of their penetration in power systems [3]. Despite the economic and environmental benefits of such sources, their intermittent nature deteriorates the power systems reliability and security status to a higher extent [4]. Hence, while uncertain generations become more significant in power systems, the necessity for a more responsive and costly reserve power increases [5]. Consequently, there is an emerging opportunity for power producers (which have fast ramping abilities) to achieve a greater economic advantage in the liberalized electricity market. In particular, WPPs could be incentivized to participate in the reserve market since the wind turbines are nowadays equipped with fast

* Corresponding author.
E-mail address: seyyedahmad.hosseiniqarehtapeh@umons.ac.be (S.A. Hosseini).

https://doi.org/10.1016/j.apenergy.2020.115973
Received 21 July 2020; Received in revised form 4 September 2020; Accepted 2 October 2020
Available online 17 October 2020

Nomenclature

Abbreviations

WPP	Wind Power Producer
JERM	Joint Day-Ahead Energy and Reserve Market
BTCS	Bi-Objective Two-Stage Chance-Constrained Stochastic
TSO	Transmission System Operator
CLRA	Confidence Level of Reserve Power Availability
TIL	Turbulence Intensity Level
BRP	Balance Responsible Party
FCR	Frequency Containment Reserve
MOP	Multi-Objective Programming

Sets and indices

ω/Ω	Scenario index/ set of scenarios
H	Set of first-stage decision variables
Ψ	Set of second-stage decision variables
k	Index of MOP sub-problem
S	Set of feasible solution space in the generic MOP problem
i	Index of the optimal Pareto solution
w	Index of wind signal in ex-post analysis
$t^{'}$	Index of balancing stage time-interval in ex-post analysis
f	Index of frequency signal
t	Instantaneous time index
j	Index of imbalance settlement period
$\tau_j^{'}$	j^{th} imbalance settlement period

Parameters

Δt	Market time unit, i.e. 1 h
λ^{Eo}	Day-ahead energy market price
$\lambda^{B\uparrow}$	Imbalance settlement price for over-generation
$\lambda^{B\downarrow}$	Imbalance settlement price for under-generation
θ	The required real-time percentage of FCR
Δf	Frequency deviation of the power system
λ^{Ro}	Day-ahead reserve power procurement price
$\lambda^{R\downarrow}$	Penalty rate regarding deviation of available capacity from the offered bid
$\lambda^{a\uparrow}$	Reserve activation price in terms of energy
$\lambda^{a\downarrow}$	Reserve activation penalty rate considering availability check
π_ω	Probability of occurrence of scenario ω
θ_ω	The activated percentage of the FCR at scenario ω
P_{min}/P_{max}	Minimum/maximum limit of WPP's generation
P_ω^q	Total available wind power at scenario ω
M	Big-M constant for mixed-integer programming
m	Small positivity tolerance in Big-M method
ε_k	Right hand side parameter of the constrained objective in k^{th} sub-problem
F_{2min}/F_{2Max}	Minimum/maximum bound of the second objective function
Q	Number of grid points in ε-constraint method
r_k	Right hand side parameter of the constrained objective, Risk, in k^{th} sub-problem
τ	Time resolution of reserve power settlement at the balancing stage (10 s)
N	Number of time-intervals at the balancing stage
$P_{t^{'},w}$	Available capacity regarding reserve market at instance $t^{'}$ for wind signal w
$\theta_{t^{'},f}$	Percentage of the called reserve at instance $t^{'}$ for frequency signal f
$\tau^{'}$	Imbalance settlement time resolution (1/4h)
$\widetilde{P}_{t,w}$	Power injected into the network for t^{th} time instance and wind signal w considering wind turbine derating
t_j	Integral bound of power to calculate the deliverable energy for j^{th} imbalance settlement period
$E_{\tau_j^{'},w}$	Available energy of wind signal w at imbalance settlement interval $\tau_j^{'}$ regarding wind turbine derating

Decision variables of BTCS model

P^{Ro}	Reserve bid regarding the day-ahead reserve market
P^{Eo}	Power bid regarding the day-ahead energy market
Π	Total revenue of the WPP in the JERM
Π^{Eo}	Revenue of WPP regarding day-ahead energy market
Π^{Ro}	Revenue of WPP regarding day-ahead reserve market
$\Pi_\omega^{E\uparrow}$	Revenue of WPP regarding over-generation at scenario ω
$\Pi_\omega^{E\downarrow}$	Revenue of WPP regarding under-generation at scenario ω
$\Delta P_\omega^{E\uparrow}$	Positive deviation of injected power at scenario ω from the offered bid
$\Delta P_\omega^{E\downarrow}$	Negative deviation of injected power at scenario ω from the offered bid
$\Pi_\omega^{a\uparrow}$	Revenue of WPP regarding reserve activation at scenario ω
$\Pi_\omega^{a\downarrow}$	Penalty for failing to activate the reserve power at scenario ω
$\Pi_\omega^{R\downarrow}$	Penalty regarding the deviation of the reserve power at scenario ω from the offered bid
$\xi_\omega\uparrow$	Binary variable regarding reserve activation at scenario ω
$\xi_\omega\downarrow$	Binary variable regarding failure to activate the reserve considering availability at scenario ω
ΔP_ω^R	Deviation of available capacity margin at scenario ω from the offered bid
P_ω^R	Available reserve power at scenario ω
P^{qo}	The total amount of day-ahead offered bids
P_ω^E	Delivered power to the energy market at scenario ω
μ_ω	Binary variable regarding the availability of sufficient power capacity
δ_ω	Binary variable regarding the status of available reserve power at scenario ω
$F_1(x)/F_2(x)$	First/second objective function of the generic MOP method
Φ	Confidence level of revere power availability
$\overline{\Phi}$	Risk of inability to provide the reserve power
P_i^{Ro}	Optimal power bid of day-ahead reserve market for i^{th} Pareto point
P_i^{Eo}	Optimal power bid of day-ahead energy market for i^{th} Pareto point

Other variables

Π^E	Total revenue of WPP regarding energy market and imbalance settlement
P^E	Real-time injected power to the network
Π^R	Total revenue of WPP regarding reserve market and balancing stage
P^R	Real-time available capacity margin
$\widetilde{\Pi}_{t^{'},w,i}^{Ro}$	Ex-post capacity procurement revenue for Pareto point i at time $t^{'}$ for wind signal w
$\widetilde{\Pi}_{t^{'},(w,f),i}^{a}$	Ex-post reserve activation revenue at instance $t^{'}$, Pareto point i, wind and frequency signal (w,f)
$\widetilde{\Pi}^R$	Total ex-post revenue of WPP in the reserve market
$\widetilde{\Pi}_{\tau_j^{'},w,i}^{E}$	Ex-post revenue of WPP in energy market for Pareto point i, settlement period $\tau_j^{'}$ and wind signal w
$\widetilde{\Pi}^E$	Ex-post total revenue of WPP in the day-ahead energy market and imbalance settlement
$\Delta\widetilde{\Pi}_n^R\%$	Normalized ex-post revenue deviation of the WPP in the reserve market
$\Delta\widetilde{\Pi}_n^E\%$	Normalized ex-post revenue deviation of the WPP in the

	energy market
$\Delta\widetilde{\Pi}_n\%$	Normalized ex-post total revenue deviation of the WPP
$\widetilde{\widetilde{\Phi}}_{\text{TIL}\%}$	Real-time inability of reserve procurement regarding each TIL in ex-post analysis

control schemes which enable them to rapidly alter their output power [6,7]. Different control techniques can be implemented, such as derating, as well as relative and absolute reserve procurement strategies. The de-rating method consists in restricting wind turbine maximum output power by a new specified upper bound, thereby creating a flexibility margin for upward regulation. The relative reserve power procurement strategy specifies a fixed percentage of the available wind power for curtailment. Finally, the absolute strategy restricts the wind turbine output power by a fixed quantity, given that sufficient power is available, to take part in the reserve market whereas the rest of the available power is allocated to the energy market [7]. The latter strategy thus prioritizes the provision of the contracted reserve power.

A possible way to tackle the imbalance cost of wind power deviation is to team up with other stable power sources, such as thermal power [8] or hydro technology [9], in order to maximize the portfolio's profit. However, coordinated bidding may not be recognized in some markets [10]. Moreover, owing to the recent developments in the wind turbines' technology, market incentives, and forecast tools, the WPPs are seeking to obtain an optimal offering strategy while acting as single GENCO owners in the electricity market [11]. Accordingly, several studies have been devoted to devising efficient tools for the participation of WPPs in the day-ahead energy market while minimizing real-time energy imbalances [12–18].

In [12] a stochastic bidding algorithm for single and dual imbalance settlement schemes is presented to enhance WPP's profit in the day-ahead energy market while minimizing the imbalance costs considering generation and price uncertainties. An optimal energy bid is obtained in [13] by reducing the commercial risk of imbalance cost using Markov probabilities. In addition, the impact of market closure delays and forecasting window lengths are studied. In [14], an hourly bidding strategy for a WPP participating in the day-ahead energy and adjustment market is proposed while controlling the risk of profit variability at the expense of a minor decrease in expected profit. In [15] an energy offering curve aiming to maximize the WPP's profit is obtained through the two-dimensional distribution of price and wind power prediction errors. The presented offer curve has greater profitability rather than the offer curve of the marginal distribution. An optimal energy bidding strategy to maximize the operating profit of a WPP in a real-time market is developed in [16], taking into account the uncertainty of other energy sources. The presented model employs a bi-level stochastic optimization scheme in which the lower-level clears the real-time market and the upper-level reduces the negative profit of the WPP. In [17], the negative impact of real-time energy deviations of WPP is mitigated by buying a quantity of energy from the intra-day reserve market which is calculated by the Cauchy-Lorentz distribution model. In [18] two types of offering strategies hedge the risk of profit variability by relying on a naïve use of power forecast and stochastic model. Interestingly, it is shown that the stochastic approach outperforms the bidding strategy based on the naïve forecast in terms of expected profit and its variability.

However, despite the potential ability of wind turbines in reserve provision, limited attention is devoted to the participation of the WPP in the JERM while reducing the imbalances that occur in real-time (for energy and reserve contributions). In [19], an analytical method is applied to increase the wind power profit by participating in the JERM. In this model, both WPP and the TSO encounter less intra-hour variations in the energy market since part of these variations are absorbed in the reserve market. However, the TSO may further suffer from the risk of real-time reserve power unavailability. Moreover, the wind turbine control strategy is neglected in their model. Thus, the obtained optimal bids and the expected revenue may not be attainable in practice. In [20], different control strategies for the allocation of energy and reserve power in the bidding strategy are taken into account. The proposed model employs market penalties and wind power uncertainties in an analytical approach based on the newsvendor problem. The optimal bidding strategy of the WPP aiming to maximize its expected profit in the JERM, based on market incentives, considering wind power uncertainty is dealt with as a stochastic programming problem in [21]. The proposed method also evaluates the impact of having better forecast information, close to the real-time stage, on WPP's offering strategy.

Despite the interesting techno-economic aspect of WPPs' participation in the JERM, the intermittent nature of their output power is a barrier for allowing them to play in the reserve market. Remarkably, market policies are shaped to ensure a competitive and liberalized environment for participation of all market players subject to the system security and reliability. Notably, reserve capacity requirement is conventionally considered as a deterministic metric, e.g. fraction of demand, the largest generator or line contingency, in the market clearing process [22]. However, such practice can impose a great cost on the power system's operation since neglecting the compromise between the system's operating cost and security of supply [22]. Moreover, such criterion leaves out the stochastic nature and underlying reliability of the committed units and, thereby could result in a substantial loss-of-load in the power system [23]. Accordingly, several approaches in the course of the past 40 years have been presented so as to integrate a probabilistic reserve constraint in the market-clearing algorithm [23]. For instance, a probability method is presented in [24] such that the reliability of reserve service, based on the probability of not meeting the load, remains fixed. The authors in [22] explicitly modeled a probabilistic reserve criterion in the unit commitment problem which properly represents the reserve capacity with respect to various risk levels. In [25], a computationally efficient unit commitment approach with a probabilistic reserve based on the full capacity outage probability distribution is presented. A pool-based market-clearing method that incorporates a hybrid deterministic-probabilistic reliability measure based on the probabilities of loss-of-load due to the single and double generation outage for scheduling the capacity services is proposed in [23].

In regard to the aforementioned efforts and, more importantly, the increased uncertainty in power systems, owing to the high penetration of renewable energy sources, the incorporation of such probabilistic reserve constraints in the electricity market could potentially tackle the problem of wind power integration in the reserve market.

Accordingly, reserve market participants should guarantee a certain confidence level of reserve power availability, determined by the TSO, in order to be considered as a reserve provider. Nevertheless, while participants ensure a certain CLRA, their real-time energy and reserve power deviations should be financially settled.

Remarkably, it should be noted that the classical offering strategy of the WPP in the market, which is merely based on the market incentives, does not ensure a firm reliability level. In other words, the WPP offers power quantities such that the income resulting from the positive incentives are greater than the negative incentives. Also, the TSO is not informed about the confidence level of the contracted bid which, in return, deteriorates the system security. Hence, this paper aims to address the research gap regarding the optimal bidding strategy of the WPP while fulfilling a required CLRA. Additionally, Table 1 briefly provides the readers with the advantages of the proposed method over the methods presented in the literature in the context of the WPP's bidding strategy.

Particularly, in this paper, firstly the remuneration and penalty mechanism of the applied JERM model while satisfying the interest of

Table 1
Advantages of the proposed strategy over the methods presented in the literature regarding WPP's bidding strategy.

References	Participation in energy market	Participation in reserve market	Control technologyof wind turbine	Integrating uncertainty of system frequency	Consideration of reserve reliability
[12–18]	✓	×	×	×	×
[19]	✓	✓	×	×	×
[20–21]	✓	✓	✓	×	×
[Proposed]	✓	✓	✓	✓	✓

system operators and the WPP is detailed. The model is formulated as a bi-objective two-stage chance-constrained stochastic framework, where the first objective is to obtain the optimal bids of WPP in the different day-ahead market floors, while the second one is to ensure the desired real-time CLRA. Additionally, the absolute reserve power procurement strategy is adapted in the model to make sure that the obtained decisions of the BTCS framework are practical with respect to the wind turbine control scheme. Therefore, the obtained efficient Pareto front provides WPP with a powerful tool to participate in JERM. To do so, a plausible set of system frequency and hourly wind speed (provided by forecasting tools) are considered as uncertain variables in the model. It should be noted that generating a set of discrete scenarios, based on the available information, for simulating the uncertainties of the influencing parameters of the model, e.g. wind speed, price, in the stochastic programming is regularly practiced in power system applications [26,27]. Then, the effectiveness of the proposed approach is properly evaluated through an extensive out-of-sample analysis containing three wind turbulence intensity levels with a high resolution, i.e. 0.1 Hz, along with the real-time system frequency data. Furthermore, the obtained results are also compared with the results of the state of the art methods to show the effectiveness of the proposed framework. Finally, the impact of market incentives on WPP's risk attitude and biding strategy is detailed.

The organization of the paper is as follows. In Section 2, the JERM framework is presented. The optimal offering strategy for the participation of WPP in JERM is detailed in Section 3. In Section 4, the ex-post analysis methodology is described. Numerical results are provided in Section 5 so as to evaluate and discuss the effectiveness and flexibility of the proposed approach. A discussion regarding the advantages and limitations of the proposed framework with respect to the state-of-the-art method is given in Section 6. Finally, Section 7 concludes the paper.

2. Proposed market framework

In the proposed framework, WPPs are considered as BRPs and are thus able to contribute to the jointly cleared day-ahead energy and reserve market. Therefore, WPPs could submit two separate bids, P^{Ro} and P^{Eo}, regarding respectively the reserve and energy markets for each period Δt of the following day. The deviations from the day-ahead scheduled bids are compensated by an imbalance settlement mechanism. Indeed, the quantity of energy fed in the system by a BRP may likely deviate from its nominated bid due to the inherent uncertainties in power generation. Therefore, the TSO applies an imbalance pricing mechanism to ensure the real-time demand-supply balance at the system level. To do so, the deviating BRP is expected to purchase its generation deficit and sell its generation surplus at the energy imbalance price. The imbalance pricing scheme varies between markets [28]. In this paper, we consider an imbalance settlement mechanism in which BRPs are discouraged to deviate from the contracted bids by means of a dual pricing. The net revenue of the BRP regarding the day-ahead energy market and imbalance settlement, Π^E, versus the injected power to the network, P^E, in this scheme is graphically shown in Fig. 1. As seen in this figure, the BRP receives a defined revenue with respect to the offered energy bid and day-ahead energy market price, λ^{Eo}. However, real-time over-generation is remunerated to the committed unit at a lower price, $\lambda^{B\uparrow}$, with respect to λ^{Eo}. Likewise, the BRP should purchase the deficit of generation at a higher price, $\lambda^{B\downarrow}$.

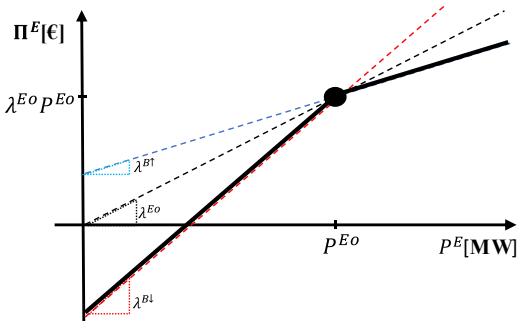

Fig. 1. Revenue obtained at the day-ahead energy and imbalance settlement versus delivered power (plain black line).

The reserve market enables the TSO to rely on power resources in order to resolve a potential system imbalance or contingency, thus ensuring systems security and stability. Therefore, producers can offer the required power-related commodities to the TSO in this market. The reserve market services are categorized by their response time and duration [29]. In this paper, the focus is around the FCR which requires the provision of power reserves in less than 30 s. The producers who offer FCR are remunerated based on the offered power in the day-ahead reserve market. However, depending on market rules, they can also get additional energy based revenue for real-time activation of FCR [30]. When it is not the case, markets should accommodate such additional energy payment in their policies, so as to incentivize WPPs to actively participate in the reserve market.

The required real-time percentage of the FCR, θ, which is automatically activated by the TSO in a decentralized way, is a function of the system frequency deviation Δf. In this regard, when a deviation is within the dead-band, $|\Delta f| \leq 0.01$ Hz, the system is considered to operate normally and no FCR service is activated. However, a specific percentage of FCR is activated for $0.01 \leq |\Delta f| \leq 0.2$ as a linear function of Δf. Then, the full power is activated for $|\Delta f| > 0.2$. This relationship between the FCR activation and the system frequency deviation is illustrated in Fig. 2. It should be noted that positive frequency deviations indicates a surplus of generation and thus a down-regulation requirement, whereas negative Δf requires the activation of upward regulation.

Concurrently, a screening scheme exists to verify the real-time availability of FCR, and penalizes the reserve providers which fail to provide the offered capacity. Accordingly, two penalty prices are considered in the proposed JERM structure in order to meritoriously remunerate the committed providers.

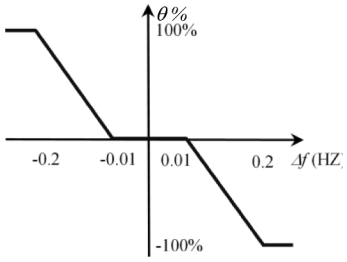

Fig. 2. Percentage of FCR activation with respect to frequency deviation Δf.

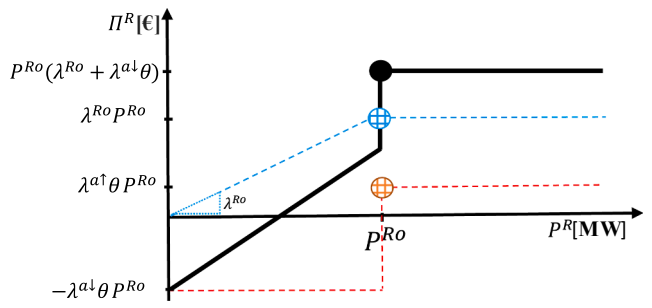

Fig. 3. Representation of the different revenues from the FCR, i.e., procurement revenue as a function of the offered FCR bid (blue), activation revenue as a function of the percentage of called reserve θ (Red), and total revenue in the reserve market as a function of the delivered FCR (black).

In the day-ahead stage, the FCR provider is paid for the offered quantity, P^{Ro} (MW) at the cleared reserve market price, λ^{Ro} (€/MW/h). However, at the balancing stage, the real-time deviations from P^{Ro}, is penalized by a specified price which is considered to be equal to λ^{Ro} is this study. Moreover, when the reserve provider fails to provide the required FCR, the unit pays an additional penalty. This adaptive mechanism ensures that the FCR provider yields no advantage regarding the activated FCR in terms of energy when it fails in the availability check. The net revenue of WPP in the reserve market, Π^R, versus the available power capacity, P^R , in this mechanism is illustrated in Fig. 3. In this figure, the dotted blue line shows the income for the real-time reserve procurement. It is seen that for $P^R \geq P^{Ro}$, the committed unit receives a constant expected revenue regarding the day-ahead offer. However, the lack of reserve power availability leads to a loss of revenue in real-time. Moreover, as shown by the dotted red line, the participant obtains a constant revenue of $\lambda^{a\uparrow}\theta\ P^{Ro}$ when it passes the availability check in real-time for reserve activation. In contrast, when $P^R < P^{Ro}$, the committed unit is penalized at a higher price factor $\lambda^{a\downarrow}\theta\ P^{Ro}$. Finally, the total revenue of WPP in real-time is obtained by adding both remuneration strategies as shown by the plain black line.

3. Offering strategy of wind power producers

The proposed BTCS framework takes advantages of a multi-objective programming approach to simultaneously optimize WPP's profit and CLRA in the JERM. The idea behind the presented framework is illustrated in Fig. 4. As seen in this figure, WPP's profit and confidence level of reserve power availability is modeled as a stochastic model, in which system frequency and wind speed uncertainties appear as the inputs of profit maximization problem while the maximization of CLRA only required wind speed uncertainty as the input. Finally, the bi-objective optimization programming allows us to illustrate the impact of the risk threshold, defined by the TSO, on WPP's revenue. The details and formulation of each objective and the applied MOP approach are further elaborated in the following subsections, i.e. 3.A-C.

3.A Objective functions and problem constraints

The first objective function Π of the proposed MOP problem aims to maximize WPP's profit in a two-stage stochastic programming framework, in which the first and second stages respectively represent the day-ahead and real-time market floors. The objective function is formulated as follows:

$$\underset{H,\Psi}{\text{Max}}\Pi = \left\{\Pi^{Eo}+\Pi^{Ro}\right\} + \left\{\begin{array}{l}\sum\limits_{\omega\in\Omega}\pi_\omega(\Pi_\omega^{E\uparrow}-\Pi_\omega^{E\downarrow}\\ +\Pi_\omega^{a\uparrow}-\Pi_\omega^{a\downarrow}-\Pi_\omega^{R\downarrow})\end{array}\right\} \quad (1)$$

The terms Π^{Eo} and Π^{Ro} respectively represent the revenue of the WPP in the day-ahead energy and reserve markets, and are given by:

$$\Pi^{\text{Eo}} = \lambda^{Eo}\Delta t P^{Eo} \quad (2)$$

$$\Pi^{\text{Ro}} = \lambda^{Ro}P^{Ro} \quad (3)$$

Then, the effect of real-time deviations from the contracted day-ahead bids on WPP's revenue is taken into account by the second term of (1). In that regard, π_ω is the probability of occurrence of scenario $\omega \in \Omega$. The energy imbalance settlement is represented by $\Pi_\omega^{E\uparrow}$ and $\Pi_\omega^{E\downarrow}$, which respectively indicate the financial compensation regarding real-time surplus and deficit of generation in scenario ω. The mathematical expression of the energy imbalance settlement, as described in Section 2 and illustrated in Fig. 1, is as follows:

$$\Pi_\omega^{E\uparrow} = \lambda^{B\uparrow}\Delta t\Delta P_\omega^{E\uparrow} \quad (4)$$

$$\Pi_\omega^{E\downarrow} = \lambda^{B\downarrow}\Delta t\Delta P_\omega^{E\downarrow} \quad (5)$$

where $\Delta P_\omega^{E\uparrow}$ and $\Delta P_\omega^{E\downarrow}$ are respectively the positive and negative power imbalances with respect to the day-ahead energy market bid of scenario ω.

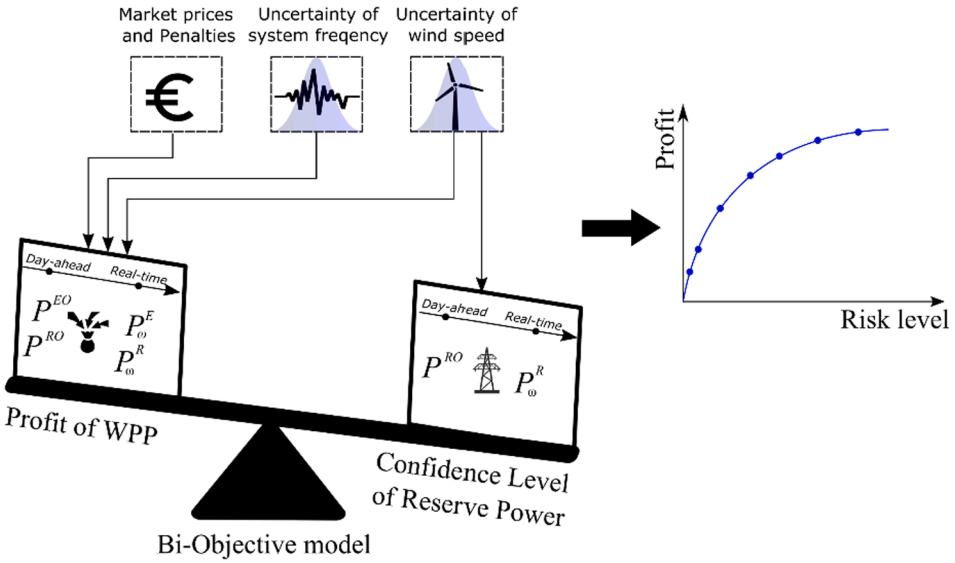

Fig. 4. Proposed bi-objective two-stage stochastic chance-constrained framework for profit maximization of WPP with respect to risk thresholds.

The last 3 elements in (1) represent the real-time balancing stage in which $\Pi_{\omega}^{a\uparrow}$ and $\Pi_{\omega}^{a\downarrow}$ respectively indicate payment and penalty for reserve activation, while $\Pi_{\omega}^{R\downarrow}$ deals for the penalty for unavailability of the FCR in scenario ω. The mentioned elements for a given θ_{ω} , as explained in Section 2 and shown in Figs. 2 and 3, are formulated as follows:

$$\Pi_{\omega}^{a\uparrow} = \lambda^{a\uparrow}\Delta t\theta_{\omega}\xi_{\omega}\uparrow \tag{6}$$

$$\Pi_{\omega}^{a\downarrow} = \lambda^{a\downarrow}\Delta t\theta_{\omega}\xi_{\omega}\downarrow \tag{7}$$

$$\Pi_{\omega}^{R\downarrow} = \lambda^{R\downarrow}\Delta P_{\omega}^{R} \tag{8}$$

where $\xi_{\omega}\uparrow$ and $\xi_{\omega}\downarrow$ are conditional decision variables, which are equal to P^{Ro} regarding the real-time availability and unavailability of the scheduled reserve power, respectively. Also, ΔP_{ω}^{R} indicate the negative deviation of the available reserve power P_{ω}^{R} fromP^{Ro} in scenario ω.

It should be noted that the model is only considering the provision of upward reserve regulation since WPP is not able to benefit from fuel-saving return in downward regulation (like the conventional units do) [19,20].

The constraints associated with the first objective function (1) are as follows:

$$P^{Eo} + P^{Ro} = P^{qo} \tag{9}$$

$$P_{min} \leq P^{qo} \leq P_{max} \tag{10}$$

$$P^{Eo} - P_{\omega}^{E} = \Delta P_{\omega}^{E\downarrow} - \Delta P_{\omega}^{E\uparrow} \tag{11}$$

$$P_{\omega}^{E} + P_{\omega}^{R} = P_{\omega}^{q} \tag{12}$$

$$P_{\omega}^{R} \leq P^{Ro} \tag{13}$$

$$P_{\omega}^{R} \leq P_{\omega}^{q} \tag{14}$$

$$P_{\omega}^{R} \geq P^{Ro} - M(1-\mu_{\omega}) \tag{15}$$

$$P_{\omega}^{R} \geq P_{\omega}^{q} - M\mu_{\omega} \tag{16}$$

$$P^{Ro} - P_{\omega}^{R} \leq \Delta P_{\omega}^{R} \tag{17}$$

$$m(1-\delta_{\omega}) \leq \Delta P_{\omega}^{R} \leq M(1-\delta_{\omega}) \tag{18}$$

$$\xi_{\omega}\downarrow \leq P_{max}(1-\delta_{\omega}) \tag{19}$$

$$\xi_{\omega}\downarrow \leq P^{Ro} \tag{20}$$

$$\xi_{\omega}\downarrow \geq P^{Ro} - P_{max}\delta_{\omega} \tag{21}$$

$$\xi_{\omega}\uparrow \leq P_{max}\delta_{\omega} \tag{22}$$

$$\xi_{\omega}\uparrow \leq P^{Ro} \tag{23}$$

$$\xi_{\omega}\uparrow \geq P^{Ro} - P_{max}(1-\delta_{\omega}) \tag{24}$$

where P^{qo} is the total bid of the WPP at the day-ahead stage for energy and reserve market which is limited by (9) and (10). The power mismatch in scenario ω is obtained by the power balance equation in (11), where P_{ω}^{E} is the power fed in the network regarding scenario ω. Eq. (12) ensures that the allocated power in the energy and reserve market does not exceed the total available power P_{ω}^{q} of scenario ω. Constraints (13)-(16) indicate the absolute control strategy of the WPP, where μ_{ω} is a binary decision variable. In this strategy, a fixed amount of reserve power is allocated to the reserve market providing that sufficient power is available, i.e. $\mu_{\omega} = 1$. However, when the available power,P_{ω}^{q}, is lower than P^{Ro}, the power is fully allocated to the reserve market, i.e.$\mu_{\omega} = 0$, such that $P_{\omega}^{R} = \min(P^{Ro}, P_{\omega}^{q})$. The negative deviation of the allocated FCR from its analogous day-ahead bid is obtained by (17). The status of ΔP_{ω}^{R} is expressed by (18), where $\delta_{\omega} \in \{0,1\}$ is equal to 0 in case of negative deviation ($\Delta P_{\omega}^{R} > 0$), and equal to 1 when no deviation from the contracted reserve power bid exists ($\Delta P_{\omega}^{R} = 0$). It should be noted that m and M are respectively the minimum and maximum bounds of the decision variable. Constraints (19)-(21) let the conditional decision variable $\xi_{\omega}\downarrow$ to be equal to P^{Ro} so as to calculate the penalty for reserve activation failure, provided that a negative deviation between the contracted and allocated FCR exist, i.e. *if* $\Delta P_{\omega}^{R} > 0$ *then* $\xi_{\omega}\downarrow = P^{Ro}$. However, constraints (18)-(20) assign $\xi_{\omega}\uparrow$ to P^{Ro} when $\Delta P_{\omega}^{R} = 0$, so as to calculate the real-time reserve activation revenue of scenario ω . It should be also noted that the first stage decision variables, $H = \{P^{Eo}, P^{Ro}, P^{qo}\}$, and the second stage variables including $\{P_{\omega}^{E}, \Delta P_{\omega}^{E\downarrow}, \Delta P_{\omega}^{E\uparrow}, P_{\omega}^{R}, \Delta P_{\omega}^{R}, \xi_{\omega}\downarrow, \xi_{\omega}\downarrow\} \in \Psi$ are non-negative continuous. Additionally, $\{\mu_{\omega}, \delta_{\omega}\} \in \Psi$ are binary decision variables of the second stage. Moreover, P_{ω}^{q} and θ_{ω} are the uncertainty sources respectively related to the available power and system frequency in scenario ω. In the same fashion as [12,18–21], it is assumed that the generation of WPP is sufficiently low in comparison with the generation at the system level, such that it is not affecting market prices (so-called price-taker assumption). Owing to certainty equivalent theory since all prices enter linearly in (1) and WPP is a price taker, the uncertainties of market prices are substituted by their expected value [20]. Additionally, it allows us to better concentrate on the risk behavior of the WPP regarding the offered power quantities in the market.

The presented objective function in (1), along with the constraints (9)-(24), define the two-stage stochastic optimization problem aiming to maximize WPP's profit in the JERM.

Then, the second objective of the proposed BTCS problem, which maximizes CLRA is formulated as follows:

$$\underset{H,\Psi}{\text{Max}}\Phi = \mathbb{P}\left(\Delta P_{\omega}^{R} = 0, \omega \in \Omega\right) \tag{25}$$

$$P_{min} \leq P^{Ro} \leq P_{max} \tag{26}$$

$$P_{\omega}^{R} \leq P^{Ro} \tag{27}$$

$$P_{\omega}^{R} \leq P_{\omega}^{q} \tag{28}$$

$$P_{\omega}^{R} \geq P^{Ro} - M(1-\mu_{\omega}) \tag{29}$$

$$P_{\omega}^{R} \geq P_{\omega}^{q} - M\mu_{\omega} \tag{30}$$

$$P^{Ro} - P_{\omega}^{R} \leq \Delta P_{\omega}^{R} \tag{31}$$

$$\Delta P_{\omega}^{R} \geq 0 \tag{32}$$

The objective function of the CLRA problem, Φ, is presented in (25), where $\mathbb{P}$ is a probability function that computes the probability of real-time reserve availability throughout the scenarios. Similar to Section 3. A, P^{Ro} is the first stage decision variable regarding the day-ahead reserve

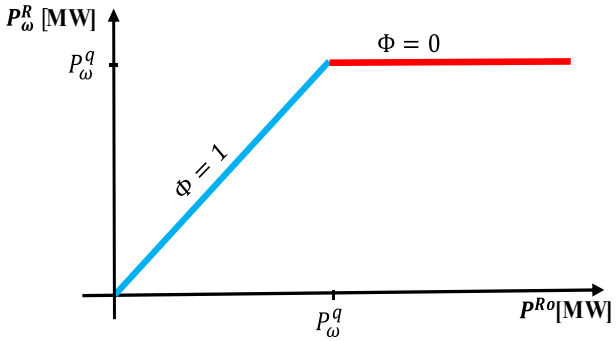

Fig. 5. Feasible solution space and objective function value of CLRA.

power bid. P_{ω}^{R} and ΔP_{ω}^{R} are the second stage decision variables, which respectively, correspond to the real-time allocated reserve power and violation of P_{ω}^{R} from the contracted bid P^{Ro}. Additionally, μ_{ω} is a binary decision variable that is equal to 1 when sufficient power regarding the contracted reserve bid is available and 0 otherwise. Also, P_{min}, P_{max} are respectively, the lower and upper power production limits of the wind turbine. The uncertainty of the available wind power and percentage of the FCR activation concerning the system frequency in scenario ω are represented by P_{ω}^{q} and θ_{ω}, respectively. Constraints (26)-(32) guarantee that the obtained solution is in the feasible space of the problem. However, it should be noted that this single-objective optimization problem does not have a unique solution in the feasible space since there is no gain to provide a likely high reserve power bid. To better illustrate this effect, let us consider a single scenario where $P_{\omega}^{q} = 2.5$MW with the probability of 100%, and $0 \leq P^{Ro} \leq 5$MW. As shown in Fig. 5, the maximum value of Φ can be obtained through various decision variables,P^{Ro} and P_{ω}^{R} within the feasible solution space as shown by a blue line.

3.B Bi-objective optimization approach:

In Multi-Objective Programming (MOP), instead of obtaining a single global optimum solution, as familiarized in single-objective problems, the concept of Pareto optimality is employed. Pareto optimality states that the performance of any objective function cannot be improved without negatively affecting the other objective functions, owing to the competing nature of objectives [31].

The weighted-sum and ε-constraint methods are the most predominant scalarization approaches among the other MOP methods in the literature of the power systems [32]. However, the ε-constraint method has some advantages over the weighted-sum approach, such as no need for normalization of the objective functions and controllability of the number of generated efficient solutions by simply adjusting a resolution parameter [32,33]. Based on the ε-constraint formulation, one objective function is chosen as the main objective,$F_1(x)$, and the other, e.g.

$F_2(x)$, is considered as inequality constraint. The generic formulation of such an approach for a bi-objective problem is as follows:

$$\underset{x \in S}{\text{Max}} F_1(x) \tag{33}$$

$$s.t. F_2(x) \geq \varepsilon_k$$

where $\varepsilon_k = F_{2min} + k(F_{2Max} - F_{2min})/Q; k = 0, \cdots, Q$

where S is the feasible region of the MOP problem and ε_k is a lower bound for $F_2(x)$. Thus, by varying ε_k in a range of minimum and maximum value of the second objective, i.e. F_{2min}, F_{2Max}, Q + 1 sub-problems are produced. Accordingly, the optimal solution of each sub-problem corresponds to a Pareto solution. However, the sub-problems with an infeasible solution should be ignored in the process of MOP. Moreover, the obtained Pareto front may contain some dominated solutions, which should be filtered out from the optimal set.

3.C BTCS Framework:

In order to plausibly investigate the effect of the risk threshold on the WPP's profit and offered power quantities in the JERM, the problem is recast as a MOP. Accordingly, WPP's profit (1) and the confidence level of reserve availability (35) are considered as the two competing objectives of the proposed MOP problem, i.e. $\underset{x \in (9)-(24)}{\text{Max}} \{(1), (35)\}$. It implies that the proposed BTCS framework concurrently maximizes the WPP's profit in a two-stage stochastic environment while ensuring a sufficient CLRA. Accordingly, Eq. (1) is considered as the primary objective function of the ε-constraint method, while the second objective (25), i.e.Φ, is treated as an inequality constraint. Additionally, the feasible space of the problem is defined by constraints (9)-(24). Also, the minimum and maximum bounds of Φ are 0 and 1, respectively. It should be noted that constraints (26)-(32) can be discarded in the MOP approach as they either are redundant or not limiting the feasible space. The compact representation of the BTCS model is finally given by:

$$\begin{aligned} &\underset{H,\Psi}{\text{Max}}\Pi \\ &\text{Constraints}(9)-(20) \\ &\Phi = \mathbb{P}\left(\Delta P_{\omega}^{R} = 0, \omega \in \Omega\right) \\ &\Phi \geq \varepsilon_k = k/Q \quad k = 0, \cdots, Q \end{aligned} \tag{34}$$

Furthermore, the primary objective function and the defined constraints (9)-(24) sufficiently limit the feasible space of the problem, thereby one decision set per CLRA is returned (as opposed to the earlier description through Fig. 5).

The probabilistic constraint in (34), which controls the real-time provision of the committed reserve, can be expressed as a chance-constrained program, and thus approximated by various approaches such as second-order cone program if the distribution of random variables follows a Gaussian function [34]. When dealing with an unstructured distribution, sampling average approximation technique accompanied by mixed integer programming can be used to estimate (34) [35–37] as follows:

$$\Phi = \sum_{\omega \in \Omega} \pi_{\omega} \delta_{\omega} \tag{35}$$

Nevertheless, in chance-constrained programming, it is more common to measure the probability of constraint violation, i.e. risk, rather than its confidence level. Therefore, the last two constraints of (34) and (35) can be reformulated as follows:

$$\overline{\Phi} = 1 - \sum_{\omega \in \Omega} \pi_{\omega} \delta_{\omega} \tag{36}$$

$$\overline{\Phi} \leq \mathrm{r}_k = k/Q \quad \mathrm{k} = 0, \cdots, \mathrm{Q} \tag{37}$$

where r_k is the analogous parameter to that of ε_k and $\overline{\Phi}$ is the one's complement of Φ, which indicates the optimal risk level regarding the tradeoff between competing objectives.

It is worthwhile noting that the proposed framework considers a single time period. However, the model can be modified by new scenarios and market settings to obtain the optimal bids of the consecutive time steps.

4. Ex-Post analysis

In this Section, we evaluate the obtained solutions of the BTCS framework using the out-of-sample approach. To that end, a set of wind speed and system frequency signals with a resolution of τ are employed so as to assess the actual revenue of the WPP. Therefore, the ex-post revenue of WPP regarding the reserve market participation including FCR procurement and activation payment along with the financial compensation in the balancing stage is described in Section 4.A. Furthermore, the ex-post revenue of WPP concerning the day-ahead energy market and the imbalance settlement is detailed in Section 4.B.

4.A. Ex-post revenue of WPP in the reserve market

In the proposed JERM market, the resolution of reserve power settlement at the balancing stage is considered to be $\tau = 10$ s. Therefore, the actual revenue of WPP for reserve procurement concerning day-ahead remuneration and real-time settlement is obtained by:

$$\widetilde{\Pi}_{t^{`},w,i}^{Ro} = N^{-1} \lambda^{Ro} P_i^{Ro} \left[1 - \mathbb{I}\left(P_{t^{`},w} < P_i^{Ro}\right)\right] \tag{38}$$

where $\widetilde{\Pi}_{t^{`},w,i}^{Ro}$ is the instantaneous revenue of WPP for Pareto optimal point $i$ at time $t^{`}$ for wind signal w. Then, P_i^{Ro} corresponds to optimal solution i within the Pareto front, while $P_{t^{`},w}$ is the available power at instance $t^{`}$ for wind signal w. $\mathbb{I}$ is the indicator function that is equal to 1

Table 2
Prices and penalties in the JERM for the base case.

λ^{Eo} [€/MWh]	λ^{Ro} [€/MW]	$\lambda^{B\uparrow}$ [€/MWh]	$\lambda^{B\downarrow}$ [€/MWh]	$\lambda^{a\uparrow}$ [€/MWh]	$\lambda^{a\downarrow}$ [€/MWh]	$\lambda^{R\downarrow}$ [€/MW]
33	36	30	40	40	60	36

when the operand in the parenthesis is satisfied and 0 otherwise. N is the number of intervals within one hour with respect to the defined resolution of the reserve market, i.e. $N = 360$.

Subsequently, real-time remuneration and settlement for reserve power activation depend on system frequency. Hence, the percentage of the called reserve as described in Fig. 2 should be calculated for each instance regarding the frequency samples.

$$\widetilde{\Pi}^{a}_{t^{'},(w,f),i} = N^{-1}\theta_{t^{'},f}P^{Ro}_{i}\left[\lambda^{a\uparrow} - \lambda^{a\downarrow}\mathbb{I}\left(P_{t^{'},(w,f)} < P^{Ro}_{i}\right)\right] \tag{39}$$

where $\widetilde{\Pi}^{a}_{t^{'},(w,f),i}$ is the actual instantaneous reserve activation revenue of WPP in which $\theta_{t^{'},f}$ is the percentage of the called reserve at instance $t^{'}$ for frequency signal f.

The total actual revenue of WPP in the reserve market, $\widetilde{\Pi}^{R}$, can be assessed using (38) and (39) for each Pareto point, i.e. risk level. It should be noted that in an ideal situation, the obtained revenue should match its corresponding expected value obtained by BTCS model, i.e. $\Pi^{Ro} + \sum_{\omega\in\Omega}\pi_{\omega}(\Pi^{a\uparrow}_{\omega} - \Pi^{a\downarrow}_{\omega} - \Pi^{R\downarrow}_{\omega})$.

4.B. Ex-post revenue of WPP in the energy market

The real-time energy imbalance should also be settled in the same fashion as explained in Section 2. In this paper, it is assumed that the BRP submits its nomination at the end of the day-ahead market with a quarter-hour resolution, $\tau^{'} = 1/4$ h. Consequently, an asymmetric imbalance tariff is imposed for BRPs who violate their nominations. Moreover, nominations of the WPP in this problem for the all intervals within one hour day-ahead market time unit is considered to be $\tau^{'}P^{Eo}_{i}$, since WPP only injects power to the network with no off-takes. Therefore, the fed-in energy to the system for each imbalance settlement interval is obtained by:

$$E_{\tau^{'}_{j},w} = \int_{t_j}^{t_{j+1}} \widetilde{P}_{t,w}dt \tag{40}$$

where $\widetilde{P}_{t,w}$ is the real-time available power injected into the network, considering the wind turbine de-rating mode, and $t_j, \forall_{j\in\{0,\cdots,3\}}$ defines the boundary of each time interval $\tau^{'}_{j}$ of the imbalance settlement process. $E_{\tau^{'}_{j},w}$ is the available energy of wind signal w at imbalance settlement interval $\tau^{'}_{j}$.

The actual net revenue of WPP resulting from the day-ahead and imbalance settlement, $\widetilde{\Pi}^{E}_{\tau^{'}_{j},w,i}$, regarding each time interval $\tau^{'}_{j}$, wind signal w and Pareto solution i is obtained as follows:

$$\begin{aligned}\widetilde{\Pi}^{E}_{\tau^{'}_{j},w,i} = {} & \lambda^{Eo}\tau^{'}_{j}P^{Eo}_{i} + \lambda^{B\uparrow}\left(E_{T_j,w} - \tau^{'}_{j}P^{Eo}_{i}\right)\mathbb{I}\left(E_{T_j,w}\right. \\ & \left.\geq \tau^{'}_{j}P^{Eo}_{i}\right) - \lambda^{B\downarrow}\left(\tau^{'}_{j}P^{Eo}_{i} - E_{T_j,w}\right)\mathbb{I}\left(E_{T_j,w} < \tau^{'}_{j}P^{Eo}_{i}\right)\end{aligned} \tag{41}$$

Finally, for each Pareto point, i.e. risk level, the total ex-post hourly revenue of WPP regarding the day-ahead energy and imbalance settlement stage, $\widetilde{\Pi}^{E}$, can be obtained using (41) which should be $\Pi^{Eo} + \sum_{\omega\in\Omega}\pi_{\omega}(\Pi^{E\uparrow}_{\omega} - \Pi^{E\downarrow}_{\omega})$ in an ideal condition.

5. Numerical results

In this Section the performance of the proposed BTCS bidding strategy is verified using a 5.3 MW wind turbine with a cut-in, rated, and cut-out wind speeds of 3, 12, and 25 m/s for participation in the JERM. In that regard, the in-sample and out-of-sample results of the proposed bidding strategy are discussed and compared to the classical bidding strategy method in Section 5.A and 5.B, respectively. Moreover, the impact of market incentives on the WPP's revenue and risk attitude for the base case is evaluated through 4 additional cases in Section 5.C. The prices and penalties associated with the presented market for the base case are shown in Table 2.

5.A. In-sample analysis

The stochastic process of the wind speed is simulated using the ARMA scenarios generation method. To do so, firstly a set of hourly mean wind speed data, available in [38], is fed into the ARMA model so as to obtain its associated statistical parameters. Then, a set of 1000 wind speed scenarios, covering the interval between the day-ahead market gate closure and the first hour of the next day, is produced by means of the estimated model. However, these numerous scenarios should appropriately be reduced, while keeping a reasonable approximation of the original distribution, in order to be practically tractable in the optimization process. Accordingly, a set of 20 wind speed scenarios, i.e. representing a sub-set of the most plausible scenarios in the original set, are collected through a scenario reduction technique based on Kantorovich distance. In this method, one scenario is chosen per iteration such that the Kantorovich distance of the main and reduced set is minimized. The iteration stops when the size of the plausible subset reaches a predetermined number. Subsequently, the selected hourly wind speed scenarios are converted to power scenarios using the static power curve of the wind turbine. Additionally, a set of 9 system frequency scenarios is also selected in the same manner so as to model the percentage of FCR activation as a stochastic process. The details of both scenario generation and reduction techniques used in this paper can be found in [39].

Both aforementioned stochastic sources along with the JERM tariffs are applied to the BTCS framework in order to obtain the optimal Pareto set. Meanwhile, a fine resolution over r_k is selected so as to reach a dense grid in the ε-constraint method, thereby sufficiently covering the entire Pareto front. Moreover, the weakly and strongly dominated solutions are filtered out in order to achieve a Pareto front that merely holds the efficient solutions. The proposed BTSC model is executed in Julia/JuMP [40] in 10.68 s on a MacBook Pro hardware set with Intel Corei5 CPU 2.3 GHz.

The resulting decisions of the BTCS framework for the first stage variables with respect to the risk of inability to provide the contracted

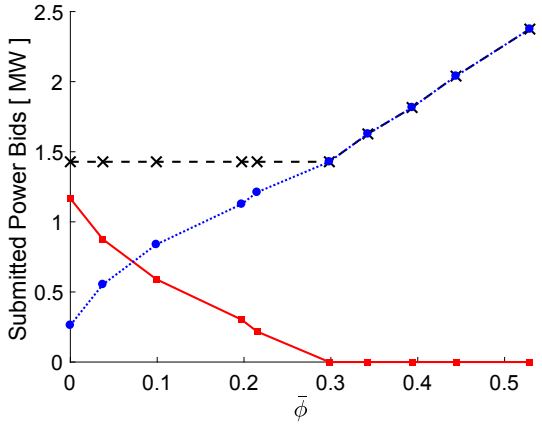

Fig. 6. First stage decision variables of the BTCS model regarding different risk levels for the base case, P^{Ro}_{i} (dotted blue line), P^{Eo}_{i} (plain red line), and P^{qo}_{i} (dashed black line).

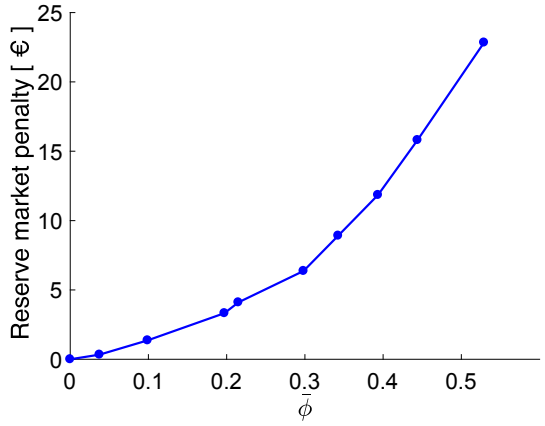

Fig. 7. The penalty paid by WPP in the reserve market with respect to the inability to provide the contracted reserve bid for the base case.

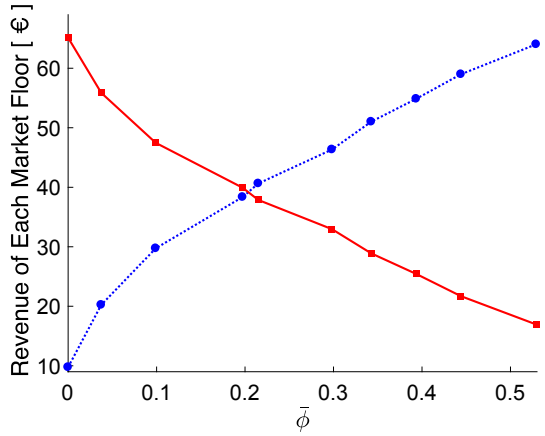

Fig. 8. The expected revenue of WPP at energy (plain red line) and reserve market (dotted blue line) for the base case.

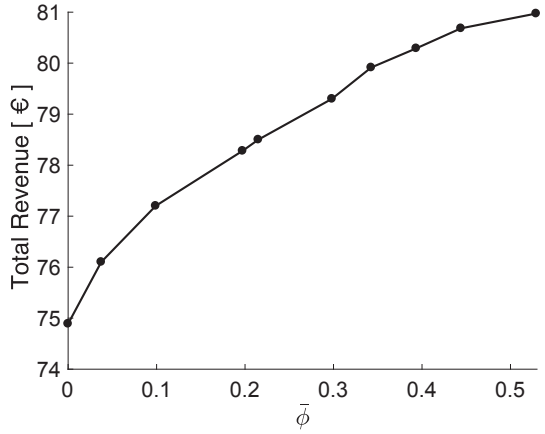

Fig. 9. The total expected revenue of WPP for participating in the JERM for the base case versus risk levels.

reserve power are shown in Fig. 6. In this figure, the horizontal axis is the expected probability of inability to provide the contracted reserve, $\overline{\Phi}$, while the vertical axis represents the scheduled power at each market floor. It can be seen that when the risk level, $\overline{\Phi}$, is between $[0, 0.3]$, WPP bids a fixed quantity of power in the JERM. As expected, when the risk level rises, WPP submits a higher power quantity in the market (and it faces thus more imbalance penalties). Likewise, risky strategies lead to a prominent share of the available power that is committed to the reserve market while a lower portion is allocated to the energy market, reflecting that bidding in the reserve market is more advantageous than in the energy market (in the studied market conditions). To get a better insight, the penalty paid by the WPP as a function of the risk threshold is shown in Fig. 7. It can be seen that the induced penalty regarding the reserve market monotonically increases with respect to the risk level.

The obtained in-sample revenue of the WPP using the proposed BTCS framework is illustrated in Fig. 8. It can be observed that the expected revenue of WPP in the reserve market (dotted blue line) is monotonically improving with respect to the permitted risk level, while the expected revenue stream of the energy market (plain red line) exhibits the opposite trend. This observation is aligned with the allocated power bids at market floors which are shown in Fig. 6. Remarkably, for risk level above 0.3, WPP still gathers revenue for its energy imbalance in real-time while not submitting any bid to the day-ahead energy market. The entire expected revenue of WPP for competing in the JERM is shown in Fig. 9 on a Pareto-efficient front in which the total expected revenue of WPP steadily grows with regard to risk levels. Accordingly, the proposed BTCS model appears to afford the WPP with a flexible tool to strategically bid in the JERM with respect to the allowed level of risk.

5.B. Ex-post analysis

As mentioned earlier, the stochastic process of intra-hour wind speed variations is approximated by an hourly mean wind speed scenario generation routine in the day-ahead decision-making process. This assumption arises from the fact that most wind speed forecasters concentrate on an hourly resolution which is thus readily accessible for WPPs. Therefore, in order to demonstrate the impact of real-time intra-hour wind speed variations on WPP's actual revenue, using the proposed BTCS tool, an extensive out-of-sample validation is performed. Accordingly, three sets of wind speed signals, embodying different TIL, i.e. 10%, 30%, and 50%, are initially produced using [41]. Each set carries 50 wind speed signals with a resolution of 0.1 Hz on a one-hour span. Furthermore, another set of system frequency realizations, with an equal dimension, is captured by employing real-world frequency deviation data available in [38]. Therefore, regarding each TIL 2500 samples are generated so as to evaluate the obtained results of the BTCS framework.

In this case, the classical bidding strategy approach [19–21], provides the WPP with the optimal bids of $P^{Eo} = 0$ and $P^{Ro} = 2.375$[MW], and revenue of 80.97 €. However, such a bid demonstrates a high-risk of unavailability in ex-post, which is equal to 0.585, 0.585, 0.569 regarding the TILs of 10%, 30, 50%, respectively. Therefore, the offered bids may even deteriorate the system's security of supply as the TSO generally considers high reliability for the reserve services.

The ex-post revenue of WPP regarding playing in the reserve and

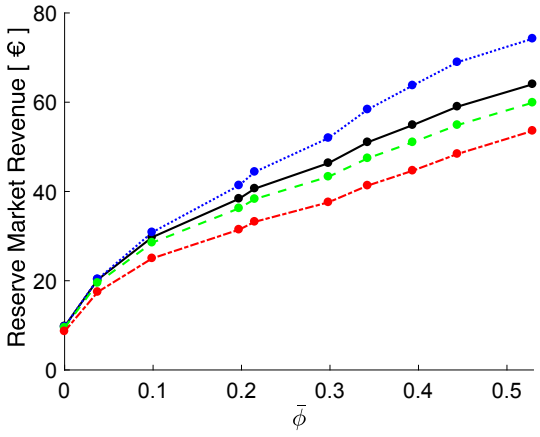

Fig. 10. The Expected revenue of WPP in the reserve market (black line) and its related actual revenue for TIL of 10% (dotted blue line), 30% (dashed green line), and 50% (red dash-dotted line) in the base case.

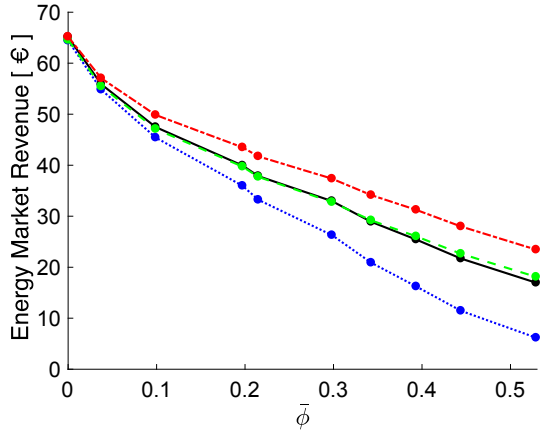

Fig. 11. The Expected revenue of WPP in the energy market (black line) and its related actual revenue for TIL of 10% (dotted blue line), 30% (dashed green line), and 50% (red dash-dotted line) in the base case.

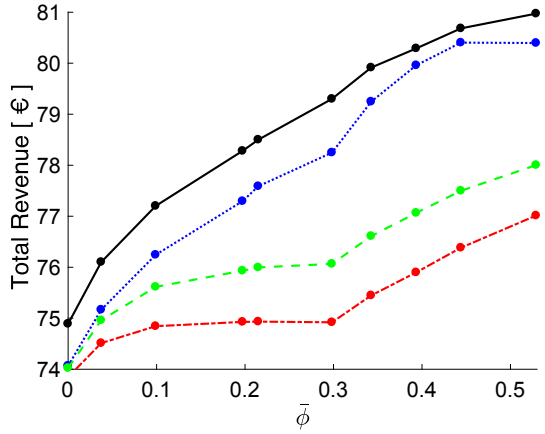

Fig. 12. The overall expected revenue of WPP in the JERM (black line) and its related actual term for TIL of 10% (dotted blue line), 30% (dashed green line), and 50% (red dash-dotted line).

energy market, based on the obtained decisions of the BTCS model, is respectively shown in Figs. 10 and 11. In these figures, the blue, green, and red styled lines respectively correspond to the TIL of 10%, 30%, and 50% while the related expected in-sample revenue is shown by a plain black line. It can be seen that for each TIL, the ex-post revenue resulting from the energy and reserve market has the same trend as its associated expected in-sample term. Nevertheless, the actual revenue of WPP in the reserve market is higher than its related expected value for a low TIL, i.e. 10%. In other words, the in-sample BTCS model overestimates the uncertainty around intra-hour wind speed fluctuations for this case, which results into conservative decisions. Conversely, for 30% TIL, the actual reserve market revenue is slightly below the expected term, while TIL of 50% is considerably lower than the expected in-sample revenue due to the inability of the WPP to offer the scheduled reserves.

More interestingly, compared to the reserve market, the real-time revenue of WPP in the energy market has an inverse behavior with respect to the increase of turbulence intensity. This aspect stems from the fact that a high turbulent wind yields more energy when the operating point of the wind turbine is in the convex region of the power curve [42–43]. Nevertheless, turbulence has a positive correlation with the fatigue of the wind turbine components [44], (thereby leading to an increase in maintenance costs) and power loss (due to the wake effect) [45]. However, it should be noticed that the static power curve of the turbine, used in this study, merely maps the mean wind speed to mean output power, and thus disregards the dynamics involved in the wind characteristics nor the turbine. In that respect, the WPP should incorporate wind turbine dynamic model in order to better assess the captured output power and component fatigue regarding the turbulent characteristics of the wind.

As seen in Fig. 11, for a low TIL, i.e. 10%, the actual revenue of WPP in the energy market is lower than the expected in-sample one while the one computed for turbulence level of 30% is really close to the expected in-sample revenue. It is also interesting to observe that the obtained revenue for a high TIL of 50% can even be higher than the expected one.

In other words, WPP may compensate for some loss of revenue by leveraging the additional available energy in turbulent wind. However, the loss of revenue in the reserve market is more substantial than the gain of revenue in the energy market concerning the increase of turbulence. As shown in Fig. 12, the total real-time revenue of WPP in the JERM concerning the expected revenue declines by the increase of turbulence level.

To gain insight into this matter, the deviation of actual revenue streams from their expected in-sample values for the different TIL is normalized by the total expected revenue of the same Pareto point. The results are detailed in Table 3. It can be seen that $\Delta\widetilde{\Pi}_n^R\%$, normalized revenue deviation of the reserve market, is between [-0.152, 12.601] for 10% TIL, [-5.118, −0.399] for TIL of 30% and finally [-13.137, −1.485] for 50% TIL. Moreover, $\Delta\widetilde{\Pi}_n^E\%$, normalized revenue deviation of the energy market, for TIL of 10%, 30% and 50% is in range of [−13.313, −0.947], [−0.758, 1.438] and [0.091, 8.015], respectively. It can be observed that when the risk level increases, the actual revenue term is getting farther from the total expected term. Additionally, $\Delta\widetilde{\Pi}_n\%$, i.e. resulting from both markets, for TIL of 10%, 30%, and 50% is in the range of [−1.328, −0.346], [−4.134, −1.501], and [−5.590, −1.394]. It is interesting to see that the wide range of $\Delta\widetilde{\Pi}_n^E\%$ and$\Delta\widetilde{\Pi}_n^R\%$ is shrunk compared to the normalized total revenue deviation $\Delta\widetilde{\Pi}_n\%$. It means

Table 3
Normalized deviation of each revenue stream regarding different TIL for the base case.

	$\Delta\widetilde{\Pi}_n\%$			$\Delta\widetilde{\Pi}_n^E\%$			$\Delta\widetilde{\Pi}_n^R\%$		
TIL $\bar{\Phi}$	10%	30%	50%	10%	30%	50%	10%	30%	50%
0.000	−1.099	−1.157	−1.394	−0.947	−0.758	0.091	−0.152	−0.399	−1.485
0.037	−1.228	−1.501	−2.089	−1.375	−0.543	1.553	0.147	−0.958	−3.641
0.099	−1.241	−2.055	−3.054	−2.664	−0.478	3.079	1.423	−1.577	−6.133
0.197	−1.260	−3.001	−4.283	−5.069	−0.260	4.556	3.809	−2.741	−8.839
0.215	−1.163	−3.192	−4.543	−5.923	−0.201	4.930	4.760	−2.990	−9.473
0.298	−1.328	−4.080	−5.524	−8.419	−0.240	5.547	7.091	−3.840	−11.071
0.343	−0.836	−4.134	−5.590	−10.027	0.355	6.556	9.192	−4.489	−12.146
0.393	−0.414	−4.017	−5.470	−11.464	0.773	7.251	11.051	−4.791	−12.721
0.444	−0.346	−3.946	−5.330	−12.690	1.172	7.807	12.344	−5.118	−13.137
0.529	−0.712	−3.668	−4.890	−13.313	1.438	8.015	12.601	−5.106	−12.905

Table 4
The real-time inability of reserve power deployment as a risk metrics concerning different TIL for the base case.

$\overline{\Phi}$	$\widetilde{\overline{\Phi}}_{10\%}$	$\widetilde{\overline{\Phi}}_{30\%}$	$\widetilde{\overline{\Phi}}_{50\%}$
0.000	0.000	0.033	0.134
0.037	0.000	0.083	0.201
0.099	0.001	0.183	0.316
0.197	0.014	0.294	0.399
0.215	0.022	0.316	0.414
0.298	0.063	0.373	0.446
0.343	0.132	0.423	0.476
0.393	0.220	0.467	0.500
0.444	0.363	0.518	0.529
0.529	0.585	0.585	0.569

that even though the model cannot fairly assess the specific revenue of each market floor with respect to the turbulence and high-risk levels, it is still able to sufficiently estimate the entire revenue of the WPP in the JERM with an acceptable range.

The obtained results of the BTCS framework regarding the second objective function, $\overline{\Phi}$, is reported in the first column of Table 4, which corresponds to the defined risk threshold by the TSO. Additionally, the out-of-sample analysis regarding the real-time inability of FCR procurement for TILs of 10%, 30, 50% ,$\widetilde{\overline{\Phi}}_{\text{TIL\%}}$, are detailed in the 2nd, 3rd and 4th columns of this Table. It is observed that the actual risk level associated with the inability to procure reserve power for 10% TIL, $\widetilde{\overline{\Phi}}_{10\%}$, is lower than the expected risk metrics, for $\overline{\Phi} < 0.529$, while greater for a high TIL, i.e. 30% and 50%. Moreover, it should be noted that setting a high-risk threshold for reserve provision by the TSO, i.e. higher than 0.5, is unrealistic, as these products should be highly reliable. Additionally, it should be further remarked that for $\overline{\Phi} = 0.529$, $\widetilde{\overline{\Phi}}_{10\%}$and $\widetilde{\overline{\Phi}}_{30\%}$is slightly higher than the case of 50% TIL. This is evident since its associated reserve power bid is equal to the deterministic value of power scenarios, i.e. slightly (3%) higher than the mean power of the generated wind signals. In other words, in turbulent wind, the possibility of reaching this rather high power-bid is higher than wind with a low TIL. Nevertheless, the actual revenue of WPP regarding this bid is still much lower than the case of 10% and 30% TIL because the deviation term ΔP_{ω}^{R} in (8) is more significant in a higher turbulent wind.

5.C. Impact of market incentives on WPP's revenue and risk attitude

In order to investigate the impact of market incentives on the WPP's revenue and its risk attitude, 4 cases regarding different market prices and penalties are presented. In each case, a specific incentive factor in the reserve market is changed while the other incentives remain unchanged as reported in Table 2. The variability of the total revenue as a function of the risk threshold is shown in Fig. 13(a)-(d). Also, similar to the base case, as discussed in Section 5.A-B, the associated expected in-sample revenue is shown by a plain black line and the ex-post revenue concerning the TIL of 10%, 30% and 50% are respectively represented by blue, green and red styled lines.

In case 1, the day-ahead reserve procurement price, λ^{Ro}, is increased to 39 $^{[€/\text{MW}]}$ in order to investigate the effect of such variation on WPP's

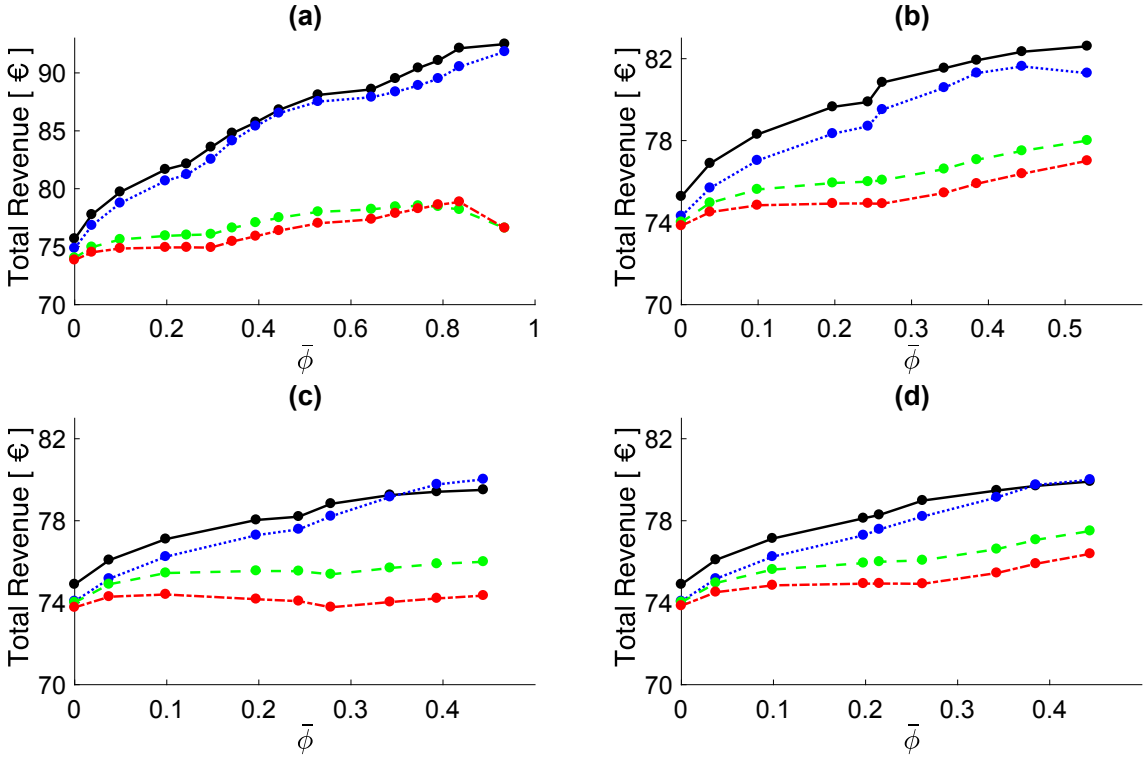

Fig. 13. (a)-(d). The impact of reserve market incentives on the risk-taking attitude and WPP's revenue including in-sample and ex-post analysis for TILs of 10%, 30% and 50%, (a) day-ahead reserve procurement price is set to 39, (b) reserve activation price is set to 88, (c) penalty regarding the deviation of the available capacity from the offered one is set to 39, (d) reserve activation penalty rate is set to 88.

Table 5
The real-time inability of reserve power deployment as a risk metrics concerning different TIL for case 1.

$\overline{\Phi}$	$\widetilde{\Phi}_{10\%}$	$\widetilde{\Phi}_{30\%}$	$\widetilde{\Phi}_{50\%}$
0.000	0.000	0.033	0.134
0.037	0.000	0.083	0.201
0.099	0.001	0.183	0.316
0.197	0.014	0.294	0.399
0.243	0.022	0.316	0.414
0.296	0.063	0.373	0.446
0.343	0.132	0.423	0.476
0.393	0.220	0.467	0.500
0.444	0.363	0.518	0.529
0.529	0.585	0.585	0.569
0.645	0.709	0.625	0.593
0.697	0.867	0.689	0.629
0.746	0.950	0.742	0.665
0.790	0.983	0.786	0.692
0.836	0.997	0.843	0.740
0.934	1.000	1.000	1.000

risk attitude and associated revenue. The single-objective solution, i.e. neglecting the risk threshold, of this case yields the expected revenue of 92.49 € regarding the optimal offered bids of $P^{Eo} = 0$and $P^{Ro} = 5.08$[MW] in the JERM. Remarkably, as the WPP does not meet any risk threshold in biding strategy, the ex-post analysis shows that, for all TILs, the WPP is never able to provide the offered capacity bid throughout the market period, i.e. $\widetilde{\Phi}_{10\%} = \widetilde{\Phi}_{30\%} = \widetilde{\Phi}_{30\%} = 1$.

On the other hand, when using the BTCS model, this favorable incentive allows the WPP to withstand a higher risk regarding the inability to provide the offered FCR service, compared to the base case, as illustrated in Fig. 13(a). As seen in this figure, the ex-post revenue of the WPP for 10% TIL stays suitably close to the in-sample results, whereas highly diverges from the expected revenue for higher TILs, i.e. 30% and 50%. Moreover, as shown in Table 5, for 10% TIL, the actual risk level, obtained by out-of-sample analysis, regarding the inability to procure the offered FCR is lower than the expected risk level for $\overline{\Phi} < 0.529$. It means that, when the defined risk threshold, indicated by the TSO, is higher than 0.529, WPP may not be able to meet this requirement in real-time. However, defining such a high-risk threshold for reserve procurement by the TSO is unrealistic as these services should be highly reliable. The real-time risk level, obtained by ex-post analysis, for high TIL, i.e. 30% and 50%, are detailed in the third and fourth columns of Table 5.

In the second case, the reserve activation price, $\lambda^{a\uparrow}$, concerning the real-time energy deployment is augmented to 88 $^{[€/MWh]}$. In this configuration, when neglecting the risk index (single-objective problem), despite WPP submits the same bids as the base case, i.e. $P^{Eo} = 0$and $P^{Ro} = 2.375$[MW], it expects an increased revenue of 82.61 € compared to the base case, 80.97 €. However, such bids demonstrate a high-risk of unavailability in ex-post, which is equal to 0.585, 0.585, 0.569 regarding the TILs of 10%, 30, 50%, respectively. Nevertheless,

Table 6
The real-time inability of reserve power deployment as a risk metrics concerning different TIL for case 2.

$\overline{\Phi}$	$\widetilde{\Phi}_{10\%}$	$\widetilde{\Phi}_{30\%}$	$\widetilde{\Phi}_{50\%}$
0.000	0.000	0.033	0.134
0.037	0.000	0.083	0.201
0.099	0.001	0.183	0.316
0.197	0.014	0.294	0.399
0.243	0.022	0.316	0.414
0.262	0.063	0.373	0.446
0.343	0.132	0.423	0.476
0.385	0.220	0.467	0.500
0.444	0.363	0.518	0.529
0.529	0.585	0.585	0.569

Table 7
The real-time inability of reserve power deployment as a risk metrics concerning different TIL for case 3.

$\overline{\Phi}$	$\widetilde{\Phi}_{10\%}$	$\widetilde{\Phi}_{30\%}$	$\widetilde{\Phi}_{50\%}$
0.000	0.000	0.033	0.134
0.037	0.000	0.083	0.201
0.099	0.001	0.183	0.316
0.197	0.014	0.294	0.399
0.243	0.022	0.316	0.414
0.278	0.063	0.373	0.446
0.343	0.132	0.423	0.476
0.393	0.220	0.467	0.500
0.444	0.363	0.518	0.529

when incorporating the allowed risk threshold in the bidding strategy, WPP is able to obtain the optimal bids with respect to the defined risk threshold to improve its revenue in the JERM, as shown in Fig. 13(b). As seen in this figure, the ex-post revenue of the WPP closely follows its expected term for TIL of 10% while further deviates for higher TILs. Moreover, as shown in Table 6, apart from the case when the allowed risk is impractically high, $\overline{\Phi} = 0.529$, the real-time FCR unavailability is below the expected threshold defined by the TSO for 10% TIL. Also, the real-time risk level, obtained by ex-post analysis, for high TILs, i.e. 30% and 50%, are detailed in the third and fourth columns in Table 6.

In case 3, the penalty regarding the deviation of the available capacity from the offered one, $\lambda^{R\downarrow}$, is increased to 39$^{[€/MW]}$, so as to study the effect of such negative incentive in WPP's revenue and risk behavior. The outcomes of the single-objective problem for such a penalty setting shows that the revenue of the WPP compared to the related solution of the base case decreases (79.50 € versus 80.97 €). More importantly, the risk of procuring such a bid is 0.363, 0.518 and 0.529 for TILs of 10%, 30% and 50%, respectively. Although, when applying the risk measure in the bidding strategy, such negative incentive, firstly, entails the WPP's decisions not to exceed a risk of unavailability higher than 0.444. Additionally, as shown in Table 7, for 10% TIL, the ex-post risk of inability to procure the offered bid is lower than the one defined by the TSO. Moreover, the out-of-sample revenue of the WPP for this situation is close to the expected term as indicated in Fig. 13(c). It can also be seen in the same figure and Table that the ex-post revenue and risk measure gets farther from the expected values regarding higher TILs.

In case 4, the reserve activation penalty rate, $\lambda^{a\downarrow}$, is increased to 88$^{[€/MWh]}$, so as to study the effect of this negative market incentive on WPP's behavior in the JERM. It should be noted that, when merely considering the WPP's profit as the objective function and disregarding the risk threshold, WPP's optimal revenue is 79.91 € which is lower than the revenue obtained by the base case. Also, the out-of-sample analysis shows that the real-time unavailability of such a bid is 0.363, 0.518 and 0.529 for TIL of 10%, 30% and 50%, respectively. Moreover, when integrating the risk level threshold in the model, the interaction of market incentives, do not allow the WPP to take any decision riskier than 0.444, as seen in Fig. 13(d). Also, it can be seen in Fig. 13 that the

Table 8
The real-time inability of reserve power deployment as a risk metrics concerning different TIL for case 4.

$\overline{\Phi}$	$\widetilde{\Phi}_{10\%}$	$\widetilde{\Phi}_{30\%}$	$\widetilde{\Phi}_{50\%}$
0.000	0.000	0.033	0.134
0.037	0.000	0.083	0.201
0.099	0.001	0.183	0.316
0.198	0.014	0.294	0.399
0.215	0.022	0.316	0.414
0.262	0.063	0.373	0.446
0.343	0.132	0.423	0.476
0.385	0.220	0.467	0.500
0.444	0.363	0.518	0.529

ex-post revenue of the WPP for 10% TIL is acceptably close to the expected term. Additionally, as detailed in Table 8, the real-time unavailability of the contracted FCR is less than the expected one (defined by the TSO). However, evidently, when the TIL increases, the ex-post revenue deviates further from the expected revenue and the WPP is not able to meet the indicated risk threshold.

Accordingly, the variation of market incentives, including the prices and penalties, directly affect the obtained revenue of the WPP. More interestingly, the interaction of these incentives defines the maximum tolerable risk regarding reserve unavailability. In particular, when the penalty rates associated with the reserve market increases, the maximum tolerable risk decrease whereas the increases in the reserve market prices allow the WPP to take a riskier decision regarding maximization of its profit. Therefore, the market incentives alone cannot limit the risk attitude of the WPP. However, by integrating the risk threshold definition in the biding strategy framework, WPP can maximize its profit while respecting the defined risk threshold.

6. Discussion

The current advancements in electricity market regulations and control mechanisms of wind turbines motivate wind power producers to participate in the joint energy and reserve market. As shown in the results Section, the classical offering strategy of WPP in the market, which is merely based on the market incentives [19–21], does not ensure a firm reliability level. In other words, WPP offers power quantities such that the income resulting from the positive incentives are greater than the negative ones. Also, the TSO is not informed about the confidence level of the contracted bid which deteriorates the system security. Therefore, their intermittent nature is a great concern of the TSO to consider them as a reserve provider, since these services are expected to be highly reliable (as conventional units). Nevertheless, regarding the advantages of the probabilistic reserve procurement metrics [22–25], discussed in Section 1, the TSO can define a risk threshold for the participation of WPP in JERM. In this way, WPP integrates the indicated risk threshold in its bidding strategy algorithm so as to maximize its profit while respecting market polices. The proposed BTCS framework illustrates the potential benefits of WPP's profit improvement while respecting a large range of confidence level which can be imposed by the TSO. It should be noted that future research should consider the dynamics of wind turbines while evaluating the expected results in ex-post. Moreover, with the increase of wind farm size in the near future, WPP could act as a price-maker, thus affecting market prices by their offered bids. Therefore, integrating market price uncertainty and performing a global sensitivity analysis based on market incentives should be considered. Finally, the scenario generation approach used in current studies which are based on hourly forecast should be improved using shorter time step (minute or even, ideally, 1- second) wind speed forecast tools so as to better assess the fluctuations of wind speed.

7. Conclusion

In this paper, firstly, a market framework, which incentivizes the wind power producer to participate in the day-ahead energy and reserve market so as to maximize its profit, is described. In this market setting, the transmission system operator also benefits by enhancing system security due to the appropriate penalty settings in the balancing stage, while specifying a new risk metric for the real-time unavailability of the scheduled reserve bids. Consequently, an advanced bidding strategy for the participation of the wind power producer in this market, considering practical constraints of wind turbine and market rules, is proposed. Then, an extensive out-of-sample validation regarding different turbulence intensity level is performed ex-post to verify the validity of the obtained results. It is shown that, in contrast with traditional models, the obtained results of the proposed bidding strategy ensure the availability of the offered bid as a probabilistic risk metric and improve the producer's revenue in the market, thereby they could practically be considered as a reserve provider. On the other hand, the risk of unavailability of the reserve power in classical approach could increase to 100%, depending on market incentives, thus threatening system's security of supply. Additionally, it is seen that with the increase of turbulence intensity level, the actual revenue of the wind power producer gets farther from the expected value. However, the deviation is still acceptable, i.e. around −5%. Nevertheless, the dynamic characteristics of the wind turbines and turbulent wind as well as intra-hour wind speed fluctuations are among the important aspects of the bidding strategy that should properly be addressed in future research works. Moreover, introducing the chance-constrained problem in the multi-objective optimization context could open up new avenues of research to apply more efficient approaches in order to obtain a higher computation efficacy and quality of the efficient frontier.

Declaration of Competing Interest

The authors declare that they have no known competing financial interests or personal relationships that could have appeared to influence the work reported in this paper.

Acknowledgements

The work is supported via the energy transition funds project "BEOWIND" organized by the FPS economy, S.M.E.s, Self-employed and Energy.

References

[1] Banshwar A, Sharma NK, Sood YR, Shrivastava R. Renewable energy sources as a new participant in ancillary service markets. Energy Strategy Rev 2017;18:106–20. https://doi.org/10.1016/j.esr.2017.09.009.
[2] Elgamal AH, Kocher-Oberlehner G, Robu V, Andoni M. Optimization of a multiple-scale renewable energy-based virtual power plant in the UK. Appl Energy 2019; 256:113973. https://doi.org/10.1016/j.apenergy.2019.113973.
[3] Abbasi MH, Taki M, Rajabi A, Li L, Zhang J. Coordinated operation of electric vehicle charging and wind power generation as a virtual power plant: a multi-stage risk constrained approach. Appl Energy 2019;239:1294–307. https://doi.org/10.1016/j.apenergy.2019.01.238.
[4] Gao W, Darvishan A, Toghani M, Mohammadi M, Abedinia O, Ghadimi N. Different states of multi-block based forecast engine for price and load prediction. Int J Electr Power Energy Syst 2019;104:423–35. https://doi.org/10.1016/j.ijepes.2018.07.014.
[5] Tsimopoulos EG, Georgiadis MC. Optimal strategic offerings for a conventional producer in jointly cleared energy and balancing markets under high penetration of wind power production. Appl Energy 2019;244:16–35. https://doi.org/10.1016/j.apenergy.2019.03.161.
[6] Wang Y, Bayem H, Giralt-Devant M, Silva V, Guillaud X, Francois B. Methods for assessing available wind primary power reserve. IEEE Trans Sustain Energy 2015; 6:272–80. https://doi.org/10.1109/tste.2014.2369235.
[7] Jeong Y, Johnson K, Fleming P. Comparison and testing of power reserve control strategies for grid-connected wind turbines. Wind Energy 2013;17:343–58. https://doi.org/10.1002/we.1578.
[8] Laia R, Pousinho HMI, Melíco R, Mendes VMF. Bidding strategy of wind-thermal energy producers. Renew Energy 2016;99:673–81. https://doi.org/10.1016/j.renene.2016.07.049.
[9] Sanchez de la Nieta AA, Contreras J, Munoz JI. Optimal coordinated wind-hydro bidding strategies in day-ahead markets. IEEE Trans Power Syst 2013;28:798–809. https://doi.org/10.1109/tpwrs.2012.2225852.
[10] Afshar K, Ghiasvand FS, Bigdeli N. Optimal bidding strategy of wind power producers in pay-as-bid power markets. Renewable Energy 2018;127:575–86. https://doi.org/10.1016/j.renene.2018.05.015.
[11] Chinmoy L, Iniyan S, Goic R. Modeling wind power investments, policies and social benefits for deregulated electricity market – a review. Appl Energy 2019;242: 364–77. https://doi.org/10.1016/j.apenergy.2019.03.088.
[12] Vilim M, Botterud A. Wind power bidding in electricity markets with high wind penetration. Appl Energy 2014;118:141–55. https://doi.org/10.1016/j.apenergy.2013.11.055.
[13] Bathurst G, Weatherill J, Strbac G. Trading wind generation in short term energy markets. IEEE Trans Power Syst 2002;17:782–9. https://doi.org/10.1109/tpwrs.2002.800950.
[14] Morales J, Conejo A, Perez-Ruiz J. Short-term trading for a wind power producer. IEEE Trans Power Syst 2010;25:554–64. https://doi.org/10.1109/tpwrs.2009.2036810.
[15] Lee D, Shin H, Baldick R. Bivariate probabilistic wind power and real-time price forecasting and their applications to wind power bidding strategy development.

IEEE Trans Power Syst 2018;33:6087–97. https://doi.org/10.1109/tpwrs.2018.2830785.
[16] Zhang Z, Chen Z. Optimal wind energy bidding strategies in real-time electricity market with multi-energy sources. IET Renew Power Gener 2019;13:2383–90. https://doi.org/10.1049/iet-rpg.2019.0058.
[17] Ghaffari R, Venkatesh B. Network constrained model for options based reserve procurement by wind generators using binomial tree. Renew Energy 2015;80:348–58. https://doi.org/10.1016/j.renene.2015.02.008.
[18] Rahimiyan M, Morales JM, Conejo AJ. Evaluating alternative offering strategies for wind producers in a pool. Appl Energy 2011;88:4918–26. https://doi.org/10.1016/j.apenergy.2011.06.038.
[19] Liang J, Grijalva S, Harley RG. Increased wind revenue and system security by trading wind power in energy and regulation reserve markets. IEEE Trans Sustain Energy 2011;2:340–7. https://doi.org/10.1109/tste.2011.2111468.
[20] Soares T, Pinson P, Jensen TV, Morais H. Optimal offering strategies for wind power in energy and primary reserve markets. IEEE Trans Sustain Energy 2016;7:1036–45. https://doi.org/10.1109/tste.2016.2516767.
[21] Soares T, Jensen TV, Mazzi N, Pinson P, Morais H. Optimal offering and allocation policies for wind power in energy and reserve markets. Wind Energy 2017;20:1851–70. https://doi.org/10.1002/we.2125.
[22] Gooi H, Mendes D, Bell K, Kirschen D. Optimal scheduling of spinning reserve. IEEE Trans Power Syst 1999;14:1485–92. https://doi.org/10.1109/59.801936.
[23] Bouffard F, Galiana F. An electricity market with a probabilistic spinning reserve criterion. IEEE Trans Power Syst 2004;19:300–7. https://doi.org/10.1109/tpwrs.2003.818587.
[24] Anstine LT, Burke RE, Casey JE, Holgate R, John RS, Stewart HG. Application of probability methods to the determination of spinning reserve requirements for the Pennsylvania-New Jersey-Maryland interconnection. IEEE Trans Power Apparat Syst 1963;82:726–35. https://doi.org/10.1109/tpas.1963.291390.
[25] Chattopadhyay D, Baldick R. Unit commitment with probabilistic reserve. 2002 IEEE Power Engineering Society Winter Meeting Conference Proceedings (Cat No02CH37309). doi:10.1109/pesw.2002.984999.
[26] Khodaei H, Hajiali M, Darvishan A, Sepehr M, Ghadimi N. Fuzzy-based heat and power hub models for cost-emission operation of an industrial consumer using compromise programming. Appl Therm Eng 2018;137:395–405. https://doi.org/10.1016/j.applthermaleng.2018.04.008.
[27] Abedinia O, Zareinejad M, Doranehgard MH, Fathi G, Ghadimi N. Optimal offering and bidding strategies of renewable energy based large consumer using a novel hybrid robust-stochastic approach. J Cleaner Prod 2019;215:878–89. https://doi.org/10.1016/j.jclepro.2019.01.085.
[28] Bottieau J, Hubert L, Greve ZD, Vallee F, Toubeau J-F. Very-short-term probabilistic forecasting for a risk-aware participation in the single price imbalance settlement. IEEE Trans Power Syst 2020;35:1218–30. https://doi.org/10.1109/tpwrs.2019.2940756.
[29] Canizes B, Soares J, Faria P, Vale Z. Mixed integer non-linear programming and Artificial Neural Network based approach to ancillary services dispatch in competitive electricity markets. Appl Energy 2013;108:261–70. https://doi.org/10.1016/j.apenergy.2013.03.031.
[30] Dabbagh SR, Sheikh-El-Eslami MK. Risk assessment of virtual power plants offering in energy and reserve markets. IEEE Trans Power Syst 2016;31:3572–82. https://doi.org/10.1109/tpwrs.2015.2493182.
[31] Hosseini SA, Amjady N, Shafie-Khah M, Catalão JP. A new multi-objective solution approach to solve transmission congestion management problem of energy markets. Appl Energy 2016;165:462–71. https://doi.org/10.1016/j.apenergy.2015.12.101.
[32] Khaloie H, Abdollahi A, Shafie-Khah M, Anvari-Moghaddam A, Nojavan S, Siano P, et al. Coordinated wind-thermal-energy storage offering strategy in energy and spinning reserve markets using a multi-stage model. Appl Energy 2020;259:114168. https://doi.org/10.1016/j.apenergy.2019.114168.
[33] Mavrotas G. Effective implementation of the ε-constraint method in multi-objective mathematical programming problems. Appl Math Comput 2009;213:455–65. https://doi.org/10.1016/j.amc.2009.03.037.
[34] Toubeau J-F, Greve ZD, Goderniaux P, Vallee F, Bruninx K. Chance-constrained scheduling of underground pumped hydro energy storage in presence of model uncertainties. IEEE Trans Sustain Energy 2020;11:1516–27. https://doi.org/10.1109/tste.2019.2929687.
[35] Ruszczynski A. Probabilistic programming with discrete distributions and precedence constrained knapsack polyhedra. Math Program 2002;93:195–215. https://doi.org/10.1007/s10107-002-0337-7.
[36] Luedtke J, Ahmed S, Nemhauser GL. An integer programming approach for linear programs with probabilistic constraints. Math Program 2008;122:247–72. https://doi.org/10.1007/s10107-008-0247-4.
[37] Kannan R, Luedtke J. A stochastic approximation method for chance-constrained nonlinear programs. ArXiv: Optimization and control 2018;12(1–37).
[38] Data Download Page. Elia. https://www.elia.be/en/grid-data/data-download-page (accessed July 2, 2020).
[39] Conejo AJ, Carrión M, Morales JM. Decision making under uncertainty in electricity markets. Int Series Operat Res Manage Sci 2010. https://doi.org/10.1007/978-1-4419-7421-1.
[40] Dunning I, Huchette J, Lubin M. JuMP: a modeling language for mathematical optimization. SIAM Rev 2017;59:295–320. https://doi.org/10.1137/15M1020575.
[41] Cheynet E. Wind field simulation. Zenodo 2020. http://doi.org/10.5281/zenodo.3817905.
[42] Kaiser K, Langreder W, Hohlen H, Højstrup J. Turbulence Correction for Power Curves. Wind Energy 2007:159–62. https://doi.org/10.1007/978-3-540-33866-6_28.
[43] Hedevang E. Wind turbine power curves incorporating turbulence intensity. Wind Energy 2012;17:173–95. https://doi.org/10.1002/we.1566.
[44] Doubrawa P, Churchfield MJ, Godvik M, Sirnivas S. Load response of a floating wind turbine to turbulent atmospheric flow. Appl Energy 2019;242:1588–99. https://doi.org/10.1016/j.apenergy.2019.01.165.
[45] Ti Z, Deng XW, Yang H. Wake modeling of wind turbines using machine learning. Appl Energy 2020;257:114025. https://doi.org/10.1016/j.apenergy.2019.114025.